Vol. 1(1), pp. 1-22, September 2022
DOI: xx.0001/AJPC2021.0207
ISSN 2021-xxxx

ASEAN Journal of Process Control

Research Article

Feedforward Artificial Neural Networks-Model Prediction Control (FANN-MPC) for Semi-Simultaneous Saccharification and Fermentation (SSSF) Bioethanol Process

Basir, N I[1]; Clara Wong Xiang Xiang[1]; Abd Syukor, S R[1] and Ahmad, Z[1,*]

[1] School of Chemical Engineering, Engineering Campus, Universiti Sains Malaysia (USM), 14300, Nibong Tebal, Penang, MALAYSIA

*Corresponding Author: chzahmad@usm.my

Academic Editor: Yudi Samyudia

Received: 3 December 2021; Accepted: 3 August 2022; Published: 1 September 2022

Abstract: The main focus of this work is on the development of nonlinear model-based control for the production of bioethanol from lignocellulosic materials following the semi-simultaneous saccharification and fermentation (SSSF) process in a fed-batch operating mode. It is observed from the current study that the SSSF process is able to give higher yield and higher ethanol concentration in comparison with the simultaneous saccharification and fermentation (SSF) process, and the separate hydrolysis and fermentation (SHF) process. In addition, working with the fed-batch operation mode, the process could be optimally controlled by externally manipulating the appropriate feed rate profiles. The SSSF process in this study, which is referred to as the SSSF 24, includes 24 hours of the pre-hydrolytic phase, and 48 hours of the SSF phase. As with other enzymatic reactions and the complexity of other reaction parameters, the non-linearity inherent to the reaction posed issues in developing efficient modelling and robust control strategies of the process. In this study, an approach has been taken to develop a mechanistic model to represent the actual dynamics of this fermentation process in a fed-batch operating mode of SSSF 24 based on a previously reported mechanistic model based on the batch operating mode. Feedforward Artificial Neural Network (FANN) model in nonlinear model predictive control (NMPC) was later developed inside the Differential Equation Editor (DEE) function block provided by Matlab™ Simulink. Data for the training, testing and validation procedure to construct the FANN were generated through randomization of the input cellulose concentration and dilution rate using the mechanistic models. The total sum of squared errors (SSE) for training and testing, and coefficient of determination, R^2, value for fed-batch operating mode are 0.0508 and 0.9998, respectively, for their best FANN architecture of 2 – 15 – 1 with 15 hidden neurons. The FANN-model predictive control (NMPC) strategy developed for the fed-batch operating mode of SSSF 24 has good setpoint tracking ability and is robust.

Keywords: Process Control, Model Predictive Control, Bioethanol, Nonlinear Model Predictive Control, Semi-simultaneous saccharification and fermentation (SSSF).

1. Introduction

One of the major issues worldwide is constantly drawn upon the everyday rising prices of fossil fuels (crude oil, coal and natural gas). As the world reserves are going to deplete anytime in the future, consumers should expect that the prices will go further escalating. According to [1], the world energy consumption, which mainly relies on fossil fuels for electricity generation will increase at an average

rate of 1.1% per year, whereby from 5.3 x 10^{14} MJ in 2006 to 7.4 x 10^{14} MJ in 2030. This is true with the increase in world population and advances in technologies. Figure 1 shows the trend of energy production and projection until the year 2050. It is seen that the energy production from renewable energy is increasing as compared to crude oil. From the daily consumption of oil in 2005 of 84 million barrels, the oil demand is projected to reach 99 million and 116 million barrels per day by 2015 and 2030, respectively [2,3].

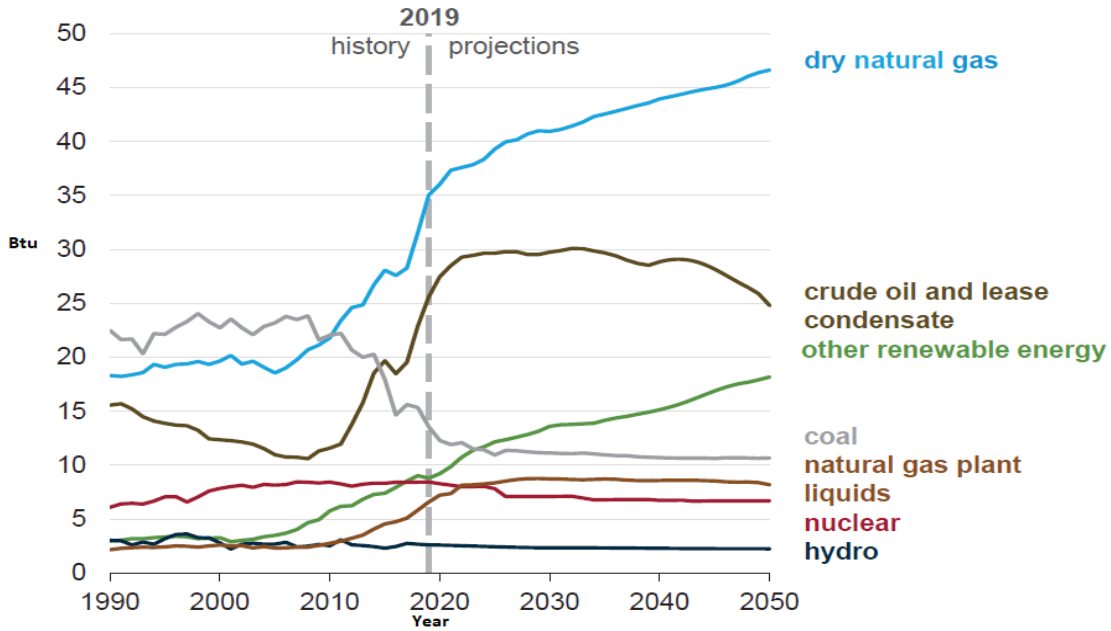

Figure 1. The curves on the trend on the energy production [3]

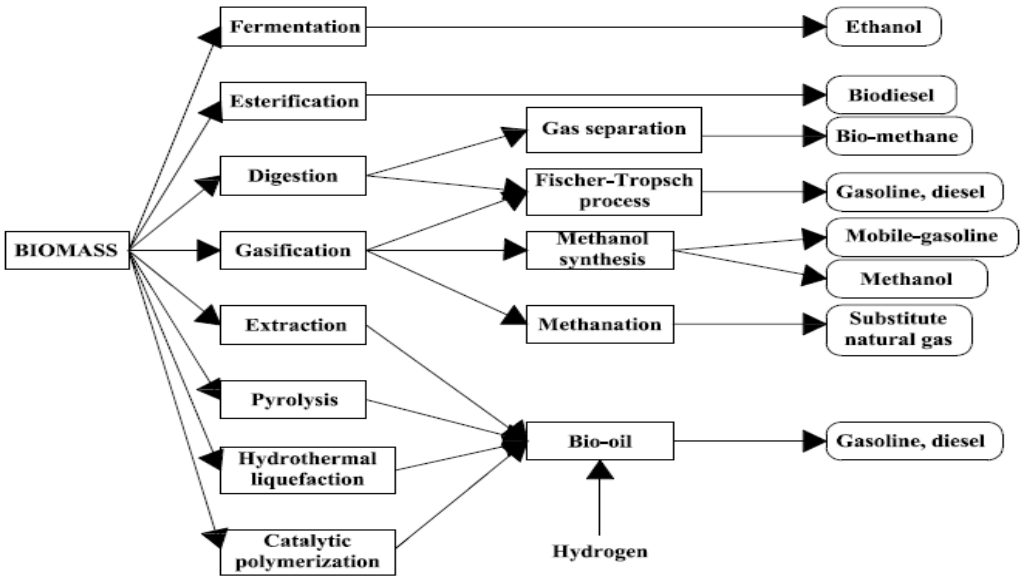

Figure 2. Biofuels from different thermochemical processes [7]

All-in-all, due to rising concern on the depletion of fossil fuels and awareness of environmental pollution, ways have been taken to search for a better renewable source of energy. One of the efforts taken to reduce greenhouse gases (GHG) emissions is the adoption of the Kyoto Protocol, an international agreement linked to the United Nations Framework Convention on Climate Change (UNFCCC). Countries that participated in Kyoto Protocol have pledged to reduce their emissions, whichever means required, even when it involves an economic cost [4]. Bioenergy has come into the picture, as it has the potential to reduce air emissions, particularly carbon dioxide (CO_2). The green concept of bioenergy involves the usage of biomass, which captures carbon from the atmosphere and later return the carbon to where it comes from when burned as fuel. Biomass includes all plant biomass

(phytomass) and animal biomass (zoomass). Biomass can be converted into different types of fuels depending on the thermal decay and chemical reformation processes used. Biomass is constituted of cellulose, hemicelluloses, lignin, small amounts of other organics and also inorganics [5,6]. The fuel products from biomass with different thermochemical processes are shown in Figure 1.

Fuel derived from biomass is called biofuels, which include bioethanol, biodiesel, and petrol/diesel additives. Among the sources of biomass for energy generation are as follows [5]:-

- Food crops, which include sugarcane, corn or maize, soybean, wheat, sugar beet and vegetable oils such as rapeseed, palm and sunflower oils.
- Hydrocarbon-rich plants, such as certain species of "laticiferous" (latex-yielding), jatropha and euphorbia.
- Waste, which includes agricultural residues (e.g. straw, vegetable/fruit peels and crop wastes), forestry waste (e.g. leaf litter and sawmill waste), food waste and biomass components of municipal solid waste [8].
- Weeds and wild growths, such as land-based plants: *mimosa* and latana, *amphibian: ipomea*, and water-based: water hyacinth, *salvini*a and *pistia* [9].
- Lignocellulosic materials, for example, the agricultural residues, woody species (e.g. willows, *Salix spp*. [10], poplars, *Populus spp*. [11], and other hardwoods [12]) and herbaceous species (e.g. switchgrass: *Panicum virgatum* [13], big bluestem, *Andropogon gerardii* [14], reed canarygrass: *Phalaris arundinacea* [15] and miscanthus: *Miscanthus spp*. [16]).

In order to make sure that the bioethanol produced is able to compete with existing fuel, such as gasoline, the cost of ethanol (biofuel) should be made as low as possible, especially from the fermentation process where the production yield is reasonably high. For this to be possible, it is necessary to develop a proper control system for bioethanol production from the fermentation process [17]. Furthermore, the dynamic of the fermentation process is very complicated due to the nature of the production process. The presence of fluctuations in the quality of feed materials will lead to changes in the kinetic behaviour of the fermentation process. These fluctuations affect the yield, productivity and conversion of the required product. It is also common that the operational conditions vary for the fermentation process [18]. Besides the variations in the quality of feed material that will cause a variation in the operational conditions, other factors such as the variations of dominant yeast in the process and reactor temperature also contribute to the variation. Thus, there is a need for the development of a proper advanced control strategy to resolve the nonlinearity of the fermentation process [19].

Nowadays, a great deal of attention is given to the application of model-based control algorithms to control biodiesel plants because of the nonlinearity inherent in some of the unit's operations such as fermentation reactors involved in the production process. The control strategies involved combining model predictive control (MPC), a member of an advanced discrete-time process control algorithm, with the capabilities of a feedforward artificial neural network (FANN). MPC has gained popularity among industrialists and academia because of its ability to accommodate both soft and hard constraints and solve multivariable control problems with the view to tracking setpoint and rejecting disturbances to the system. Integrating the development of a FANN model-based control as a nonlinear model in MPC is beneficial in terms of computational cost reduction and also in increasing the production capability (yield). Not only the production cost is able to be reduced, but there are also advantages of the proper control system in terms of waste minimization, and optimum energy consumption [20,21]. These features of FANN-MPC make it suitable for regulating a fermentation process occurring in a bioethanol reactor and can also be applied to other unit operations in a biodiesel plant that possesses a nonlinearity tendency.

The paper is organised as follows. Section 2 presents the methodology which covers the case study, mechanistic model development, FANN model development and FANN model predictive control, followed by the result and discussion in Section 3. Finally, Section 4 concludes this paper.

2. Methodology

In this section, the case study, mechanistic model development, feedforward artificial neural network (FANN) model development and validation and model predictive control (MPC) application were presented.

2.1. Case study: Semi-simultaneous Saccharification and Fermentation (SSSF 24)

The focus of this paper is on the development of the control strategy for the semi-simultaneous saccharification and fermentation (SSSF 24) process with the utilization of mechanistic equations derived in [22]. SSSF 24 were studied which included a 24 hours pre-hydrolytic phase and a 48 hours simultaneous saccharification and fermentation (SSF) phase. A mechanistic model under fed-batch operating of the SSSF 24 process was developed based on Shen and Agblevor [22] following their experimental studies. For the mechanistic model of the continuous operating mode of SSSF, two reactors were utilized, one for the pre-hydrolysis process and another for the SSF process. The model for fed-batch operating mode, which was an intermediate of the batch and continuous operating modes, was of prime concern in this study. In the fed-batch operation mode, the reactants are added continuously to the reactor, unlike the batch operating mode where all reactants are present at the beginning of the reaction or unlike the continuous mode where reactants are added and products are removed continuously to achieve a steady state condition. Utilizing the fed-batch mode of operation, the reaction processes could be optimally controlled by externally manipulating the appropriate feed rate profiles which cannot be achieved through the batch and continuous operating modes and would be crucial to processes such as in the production of high-added value products when significant substrate inhibition or catabolite repression might occur.

2.2. Development of Mechanistic Model Semi-simultaneous Saccharification and Fermentation (SSSF 24)

The mechanistic equations for the model of fed-batch operations of the intermediate of both SSF and SHF called the SSSF process developed as in [22]. The development of the batch model was more for model verification purposes, while the fed-batch model was the primary objective of this study. The development of model predictive control (MPC) will be based on the latter model. The SSSF 24 process, in particular, is referred to as the process models simulation as it gave the highest productivity. The mechanistic models for the fed-batch were constituted of ordinary differential equations (ODEs), which include the kinetic rates that describe the changes of products and by-products of the SSSF process. Details of the methodology for the development of the mechanistic equations can be found in [22]. The differential equations extracted from their work are inserted into the Differential Equation Editor (DEE) function block provided by Matlab™ Simulink. The DEE is one of the solver's functions provided by Matlab™, which implements Runge-Kutta methods with variable step sizes to solve differential equations. These solvers include the ode25, ode45, and ode113. For this study, the ode45 function is chosen. Ode45 is a non-stiff and medium-order solver that is fast and accurate. Ultimately, the process models are able to predict the bioethanol concentration for different values in input variable(s).

2.2.1. Fed-Batch Operating Mode

In a fed-batch operation mode of SSSF 24, cellulose is continuously fed into the culture at a flow rate of F (dm^3/h). However, no output is withdrawn from the reactor. The term dilution rate, D (h^{-1}), is introduced.

$$D = \frac{F}{V_2} \tag{1}$$

where, V_2 refers to the liquid volume in the SSF process reactor. The process model for the fed-batch operating mode of SSSF was simulated with the assumptions of: -

- The parametric values for the fed-batch process were the same as from the batch process.
- With the substrate conversion, x, taken as 0.58 following the highest conversion reported in [22] for hydrolysis reaction within a period of 24-h, the initial concentration of cellulose entering the SSF period, C_1 was obtained through the equation below:

$$C_1 = C_0 \times (1 - x) \tag{2}$$

- The constant value of k_7 is calculated from the equation below:

$$k_7 = \frac{\frac{e_0}{e-1}}{e_0 \times 48} \tag{3}$$

- The initial enzyme concentration entering the SSF period, e_1 was obtained through the following equation:

$$e_1 = \frac{e_0}{1+k_7' e_0 t} \quad (4)$$

where, the pre-hydrolysis reaction time, t = 24 hours.

The mechanistic models used are to be examined for their accuracy and compatibility to represent the dynamics of the actual process. The validation of the model was carried out by comparing the output responses obtained from the mechanistic models with the responses obtained through experimental studies performed in [22]. Since their experimental works were on the batch operating mode of SSSF 24, only the mechanistic process model of batch operating mode was used for verification purposes.

2.2.2. Feedforward Artificial Neural Networks (FANN) Model for Semi-simultaneous Saccharification and Fermentation (SSSF 24)

The main goal of this study is to develop an accurate process model and control strategy for the production of bioethanol in order to maintain a certain (optimum) concentration of ethanol produced from the SSSF 24 process. This control scheme can be achieved through the manipulation of the correct input variable(s) and the correct selection of output variable(s). During the process to simulate the mechanistic model of bioethanol concentration for the bioethanol fermentation process, some higher effective variables are chosen as the input variables of model-based control.

Referring to Figure 3 on the extractive alcoholic fermentation process, which can be associated with the SSSF 24 of the bioethanol production system under the current study, the inputs include the cell concentration, *X(t)*, feed flow rate, *F(t)*, substrate/cellulose concentration, *S(t)*, bioethanol concentration, *P(t)*, and fermentation time, T_F [23]. As described in the previous section, the yield and rate of enzymatic hydrolysis can be further improved by various designs of fermentation reactors and different plant configurations. Initially, a multi-input multi-output (MIMO) model was developed according to the mechanistic equations developed by Shen and Agblevor [22].

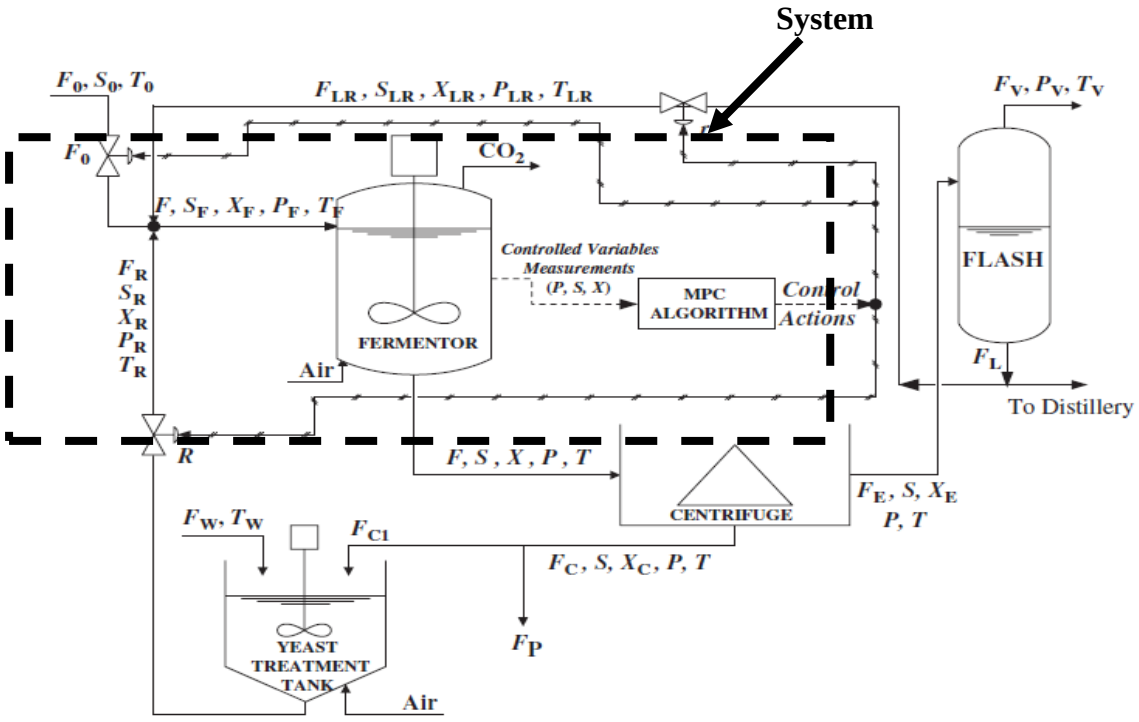

Figure 3. Process Flow Diagram of an Extractive Alcoholic Fermentation Process [23].

However, for this study, only selected input parameters and output parameters were selected as shown below for fed-batch operating mode:

(i) Manipulated Variables (*u*): Current value cellulose concentration, *C(t)*, current value of dilution rate, *D(t)*, and past value of bioethanol concentration, *E(t-1)*.

Control Variables (*y*): Bioethanol concentration, *E*(*t*).

Thus, the dynamic model for the batch operating mode can be expressed as follows:

$$\widehat{E(t)} = f(C(t), D(t), E(t-1)) \quad (5)$$

where, $\widehat{E(t)}$ is the predicted bioethanol concentration at time *t*, *E(t)* is the actual bioethanol concentration at time *t*, *C(t)* is the cellulose concentration at time *t*, and *D(t)* is the dilution rate at time *t*.

(ii) Manipulated Variables (*u*): Current value cellulose concentration, *C*(*t*), and past value of bioethanol concentration, *E*(*t-1*).

Control Variables (*y*): Bioethanol concentration, *E*(*t*).

Thus, the dynamic model for the batch operating mode can be expressed as follows:

$$\hat{E}(t) = f(C(t), E(t-1)) \quad (6)$$

where, $\hat{E}(t)$ is the predicted bioethanol concentration at time *t*, *E*(*t*) is the actual bioethanol concentration at time *t*, and *C*(*t*) is the cellulose concentration at time *t*.

(iii) Manipulated Variables (*u*): Current value of dilution rate, *D*(*t*), and past value of bioethanol concentration, *E*(*t-1*).

Control Variables (*y*): Bioethanol concentration, *E*(*t*).

Thus, the dynamic model for the batch operating mode can be expressed as follows:

$$\hat{E}(t) = f(D(t)\ E(t-1)) \quad (7)$$

where, $\hat{E}(t)$ is the predicted bioethanol concentration at time *t*, E(t) is the actual bioethanol concentration at time *t*, and *D*(*t*) is the dilution rate at time *t*.

Thus, multi-input single-output (MISO) neural models representing the sub-systems of the batch and fed-batch modes of the SSSF 24 process were developed. For the fed-batch operating mode, a term dilution rate was introduced. Dilution rate refers to the ratio of feed flow rate against culture volume. Three different conditions were studied for the fed-batch operating mode: (i) with three inputs; (ii) with the current value of cellulose concentration, and past value of bioethanol concentration as inputs; and (iii) with the current value of dilution rate, and past value of bioethanol concentration as inputs. Some of the significant notations on Figure 3 include: F = feed flow rate; S_F = substrate/glucose concentration at feed; X_F = cell concentration at feed; P_F = ethanol concentration at feed; T_F = fermentation time; P = ethanol concentration at output; S = substrate/glucose concentration at output; and X = cell concentration at output. The area highlighted with a thick dash line was the system boundary appropriate for this study. These include the feed line, fermentor, the to-be-developed MPC strategy, and the control line that follows.

A feedforward artificial neural network (FANN), with a backpropagation algorithm, was selected as the network structure for the neural model. Randomization on the input parameters was used to generate nine batches of data for the fed-batch operating mode of SSSF 24. These batches of data were distributed with approximately 70 – 80 % were used in the training and testing steps and the rest of the data were used for validation of the network model. Before proceeding to the network development, a scaling procedure to normalize the training data set to zero mean and unity standard deviation, which was able to cope with the different magnitudes in the input and outputs was performed [24]. The network was trained using inputs from the preprocessing of the original training data set [25]. Normalization of the training data will rapid up the network training. The following equation was used for the normalization procedure.

$$y' = (x_i - x_{mean}) \times \frac{y_{std}}{x_{std}} + y_{mean} \quad (8)$$

The training data set was used to adjust the weights of all connecting nodes until the desired error level was reached. The training was done according to the Levenberg-Marquardt (LM) algorithm.

The LM algorithm is an iterative technique, which is able to locate the minimum of a function that is expressed as the sum of squares of nonlinear functions [26]. After training, another two batches of data were used to test the network, which is known as the testing step.

2.2.3. Validation of Feedforward Artificial Neural Networks (FANN) Model

The final procedure was to validate the FANN model performance. New data sets or unseen data, which were unknown to the network, were used to validate the network. The FANN performance was analyzed through the sum of squared errors (SSE) performance function and the coefficient of determination (R^2) which can be calculated after determining the sum of squared total (SST). The SSE performance index, which was selected as the objective function, can be calculated using the below equation. The value of the objective function was required to be minimized in order to produce the prediction output as similar as possible to the known output data.

$$SSE = \sum_{k \in data\ set}(y(k|k-1) - y(k))^2 \quad (9)$$

$$SST = \sum_{k \in data\ set}(y(k|k-1) - \bar{y}(k))^2 \quad (10)$$

$$R^2 = 1 - \frac{SSE}{SST} \quad (11)$$

where $y(k \mid k\text{-}1)$ refers to the output of the model for the sampling instant k calculated using signals up to the sampling instant *k-1*, and $y(k)$ is the real value of the process output variable collected during the identification experiment while and $\bar{y}(k)$ is the mean value of the collected process output variables.

It is crucial to have a network with very good generalization capability. One way to obtain a network with good generalization capability is to choose a structure with a sufficient number of input, hidden layers, hidden nodes and the output [27], which assure that the FANN learns the training data and then optimizes the topology of the network until the best generalization properties are achieved. The preferable network structure shall have a small SSE value and a high R^2 (~1.0). However, in this study, the network topology with one single hidden layer was chosen. To determine the number of hidden neurons in the hidden layer, a cross-validation technique was adopted where the neurones were varied from 1 to 20 and the network with the best performance in terms of SSE and R^2 was selected as a final model. Once the FANN model structure is identified, it can be used as an internal model in the FANN-MPC algorithm.

2.3 *Feedforward Artificial Neural Networks Nonlinear Model Predictive Control (FANN-MPC)*

In this study, feedforward artificial neural network–model predictive control (FANN-MPC) was developed for the fed-batch SSSF 24 of the bioethanol production system. The FANN-MPC function block can be accessed in the Matlab™ Simulink environment, through the Neural Network Toolbox software. In brief, this controller works by employing the neural network model of a nonlinear plant for the prediction of future plant performance. It calculates the control input that will optimize the plant performance over a specified future time horizon.

The neural network model of the fermentation reactor is to be determined before proceeding with the control algorithm. This procedure is known as the system (plant) identification step as described in section 2.2.2. In this initial step, a neural network that was able to exemplify the dynamics of the fed-batch mode of SSSF 24 was developed. With the reference to Figure 4, the prediction error (Error) between the plant output and the neural network output is used as the neural network training signal. The neural network plant model uses past inputs and past plant outputs to predict future values of the plant output. The dynamic model for the batch operating mode can be expressed as follows:

$$\hat{E}(t) = f(D(t\text{-}1)\ E(t\text{-}1)) \quad (10)$$

where, $E\hat{}(t)$ is the predicted bioethanol concentration at time t, $E(t)$ is the actual bioethanol concentration at time t, and $D(t)$ is the dilution rate at time t.

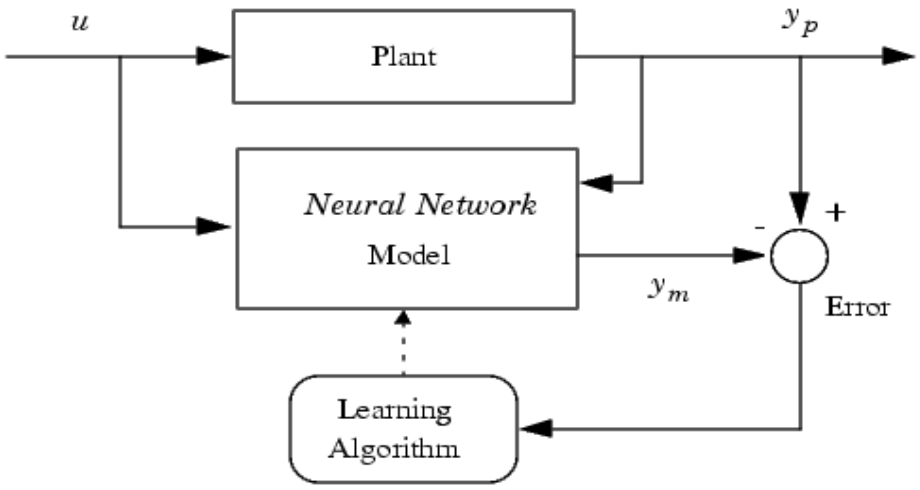

Figure 4. Block diagram on the process of working of NNMPC [28].

In the plant identification stage, the network architecture, training data generation, and network training can be performed. The training of neural networks was done offline. The neural network model for the fed-batch operating mode of SSSF 24 obtained in the FANN modelling stage can be imported into the FANN-MPC. However, in this study, a new neural network was developed by embedding the fed-batch process model that has been simulated earlier in the Matlab Simulink environment to obtain the network training data. The network training according to the plant process model was expected to give a more precise and accurate network to represent the dynamics of the plant. The structure of the neural network plant is shown in Figure 5. The system input is denoted by *u*, the plant output is y_p, and the neural network output is y_m. The blocks TDL are the tapped delay lines that store past values of the input signals, $IW^{i,j}$ is the weight matrix from the input number *j* to the layer number *i*. $LW^{i,j}$ refers to the weight matrix from layer number *j* to layer number *i* [28].

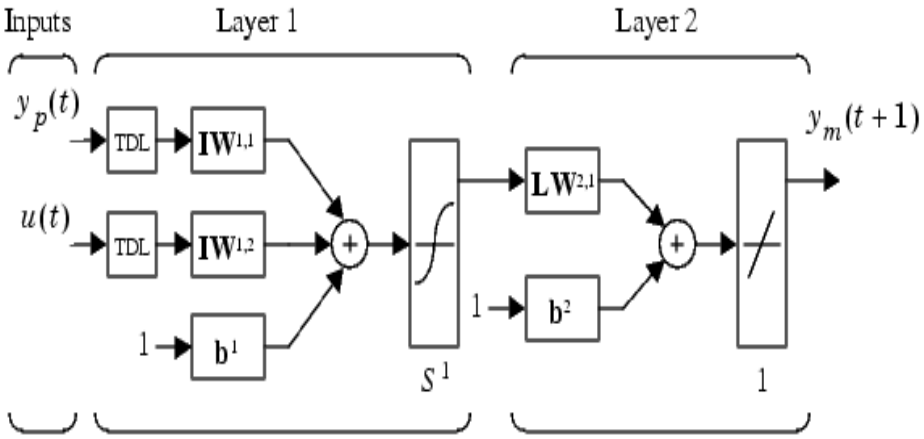

Figure 5: Structure of the neural network plant model [29].

The neural network model obtained acts as a predictor that will predict the plant response over a specified time horizon. A numerical optimization program will in turn use these predictions to determine the control signal that minimizes the performance criterion over the specific horizon. The performance criterion or the objective function, ϕ is calculated with the following equation [29]:

$$\varphi = \sum_{j=N_1}^{N_2}\left(y_r(t+j) - y_m(t+j)\right)^2 + \rho \sum_{j=1}^{N_u}\left(u'(t+j-1) - u'(t+j-2)\right) \qquad (11)$$

where, N_1 is the minimum prediction horizon, which is fixed at 1 by Matlab, N_2 is the maximum prediction horizon, N_u is the control horizon, *j* is the prediction parameter, y_r is the desired response, y_m is the network model response, *u'* is the tentative control signal, and ρ is the weighting parameter that determines the contribution that the sum of the squares of the control increments has on the performance index.

Figure 6 shows the block diagram in the FANN-MPC process with an online application to control the response of the plant. The 'Controller' refers to the neural network plant model together with an optimization block. The optimization block functions to determine the values of *u'* that minimize *j*. Later, the optimal u value is input to the plant. The NMPC function block, previously known as the 'Controller' in Figure 6, offers the user to ability to adjust the values of the tuning parameters, which include the N_2, N_u, ρ, and α until the controller is able to give a desirable performance. The search parameter, α, is used to control the optimization. It determines how much reduction in performance is required for a successful optimization step.

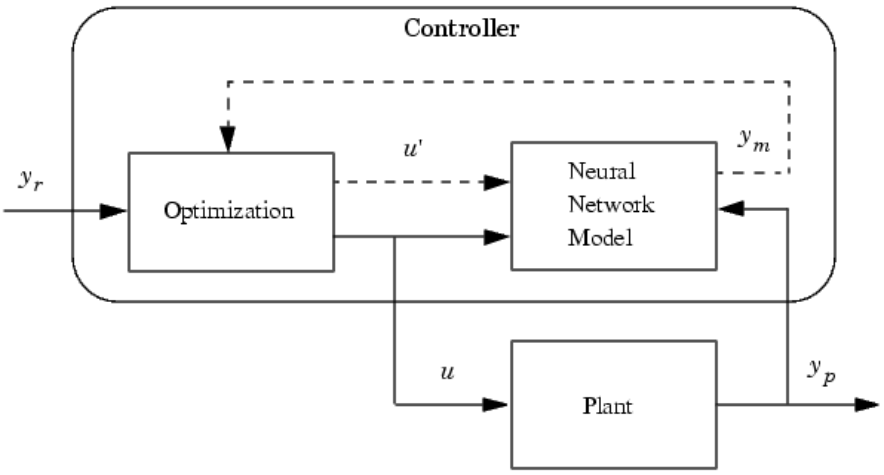

Figure 6: Block diagram on the online application of controller (FANN-MPC) [29].

3. Results and Discussion

3.1. Mechanistic Model: The Fed-Batch Operating Mode of SSSF 24 of Bioethanol Production

For the fed-batch operating mode, continuous feed of substrate is introduced into the culture, but without any extraction out from the system. There are two manipulated variables for the fed-batch operating mode: the inlet cellulose concentration; and the dilution rate. The dilution rate, *D*, was used to describe the rate of change between the flow rate of cellulose, *F* (dm^3/h), and the liquid volume in the fermentor, R_2 (dm^3). The process model for the fed-batch operation is shown in Figure 7. According to the findings in [22], the dilution rate influences ethanol concentration.

Figure 8 shows the relationship between dilution rate, ethanol, glucose and cell concentrations, and productivity in the continuous operation of SSSF 24. It is seen that ethanol concentration was dependent on the dilution rate. Ethanol concentration is highest at a lower dilution rate and lowest at a high dilution rate. A simulated best fit curve for the variation in bioethanol concentration against different dilution rates for the fed-batch operation of the SSSF 24 process was plotted in Figure 9 and Figure 10. The change in bioethanol concentration with different dilution rates for the fed-batch operating mode was investigated. The best optimum dilution rate is obtained in the range between 0.01 – 0.04 h^{-1} with the highest bioethanol concentration approximately attained being at 16.70 g/dm^3. The bioethanol concentration decreased with an increase in the dilution rate. The simulation study was conducted beyond the washout point of 0.4 h^{-1}, which was mentioned in[22] in order to check the behaviour of the bioethanol concentration. It is observed that the bioethanol concentration continues to decrease after the washout point. At the dilution rate approaching 1.0 h^{-1}, the bioethanol concentration attained is as low as 0.029 g/dm^3. Therefore, in the MPC development, the dilution rate that act as feed to the fed-batch reactor and which formed the concentration profiles in the reaction was chosen as the manipulated variable for the plant.

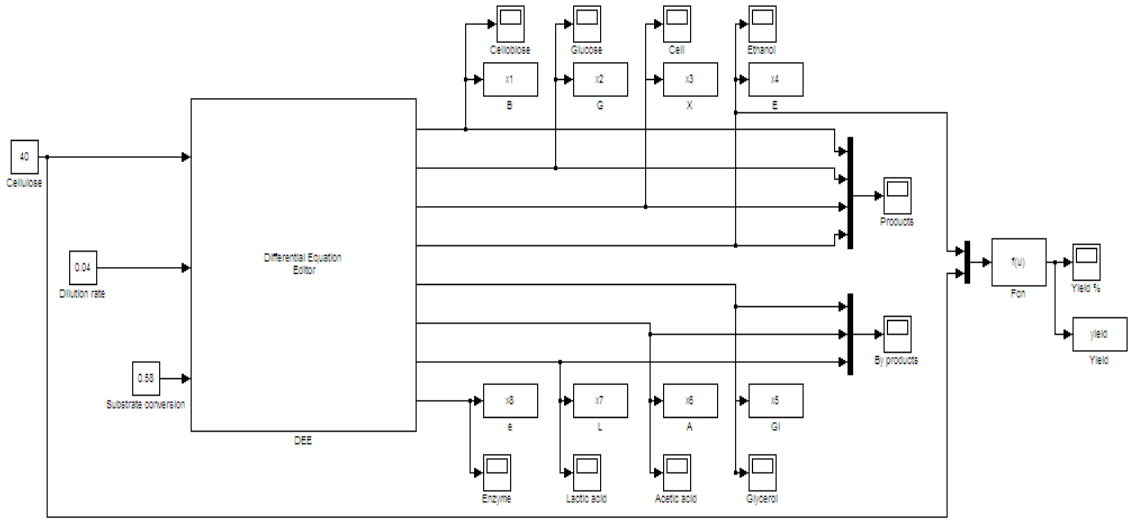

Figure 7. Fed-batch operating mode of SSSF 24 of bioethanol production.

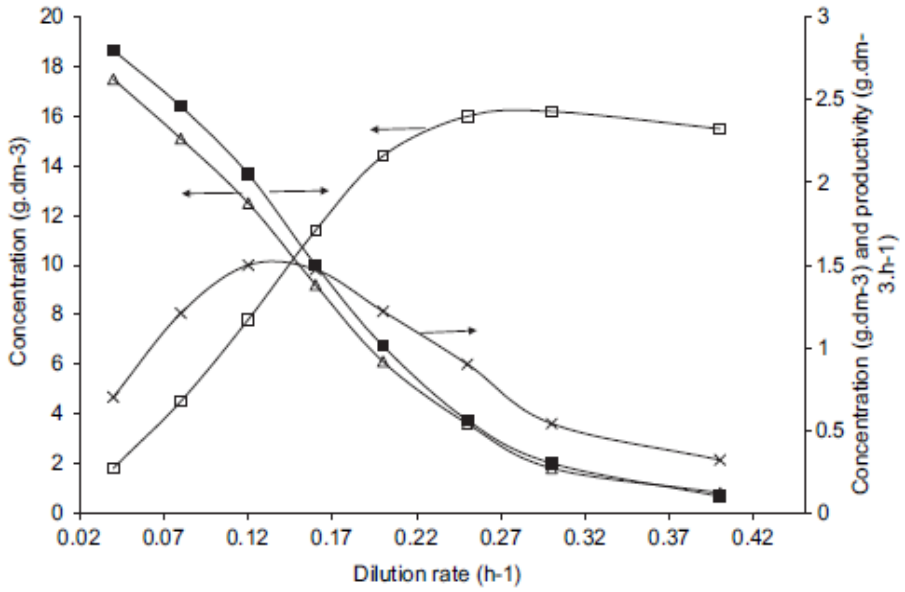

Figure 8. Variation in ethanol, glucose and cell concentrations with different dilution rates in the continuous operation of SSSF 24. Ethanol concentration is denoted by (Δ), glucose concentration is denoted by (□), productivity is denoted by (x), and cell concentration is represented by (■) [22].

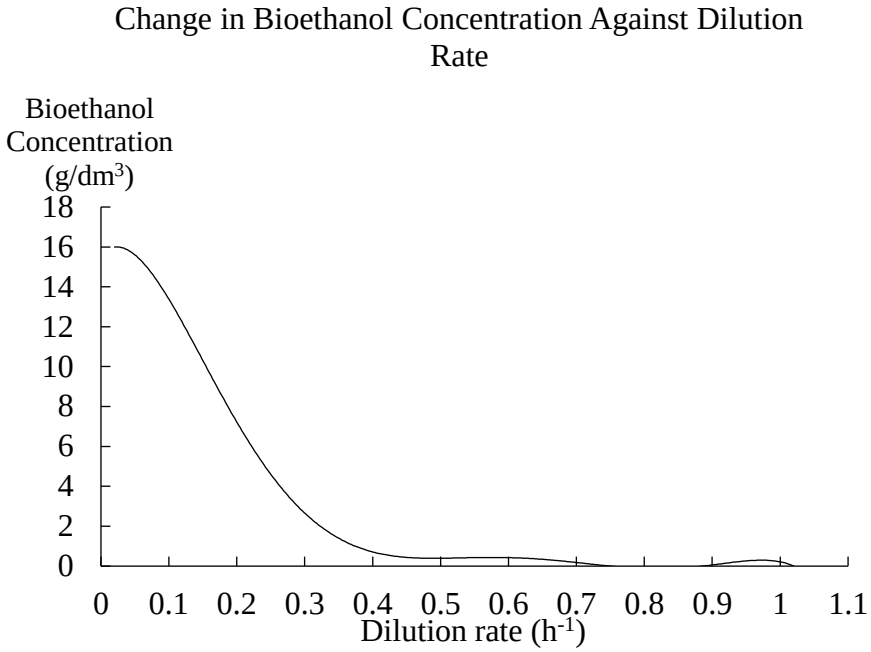

Figure 9. Simulated plot on the variation in bioethanol concentration with different values of dilution rate in the fed-batch operation of SSSF 24.

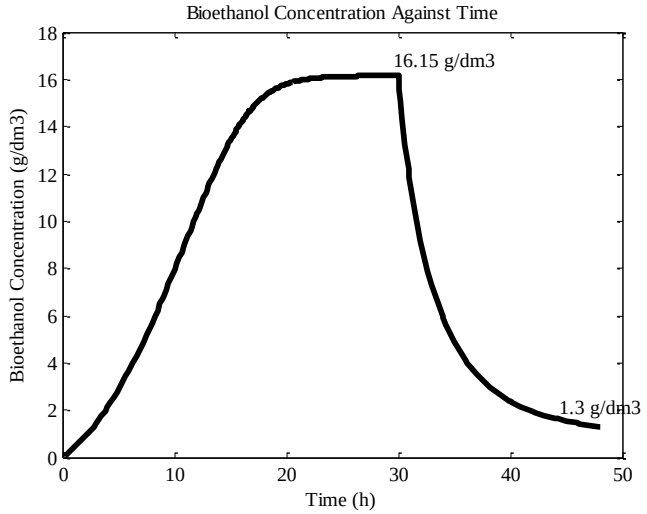

Figure 10. Response of bioethanol concentration from a step change at the time, t = 30 hours, from an initial D of 0.04 h^{-1} to D = 0.4 h^{-1}.

3.2. Mechanistic Model Validation

In order to verify the process models simulated, the results for the batch operation were compared with the experimental and simulated results obtained by [22]. The results are compared in terms of the changes in cellobiose, glucose, ethanol and cell concentrations with time. The results obtained by [22] are shown in Figure 11 while Figure 12 shows the responses from the simulated batch operation process model. At a steady-state, under the same process conditions, the bioethanol concentration from the model developed is 15.9678 g/dm^3 (approx. 16 g/dm^3) and the yield is 70.3084%, while the ethanol concentration obtained in [22] is 16.0 g/dm^3 and the theoretical yield is 70.5%. The cell concentration is about 5.4 g/dm^3 at a steady state. Figure 13 shows the yield from the batch operation process model. It is shown that the simulated model or mechanistic model developed is similar to or in agreement with the model developed in [22] with a small error of less than 1 % for bioethanol concentration and yield respectively.

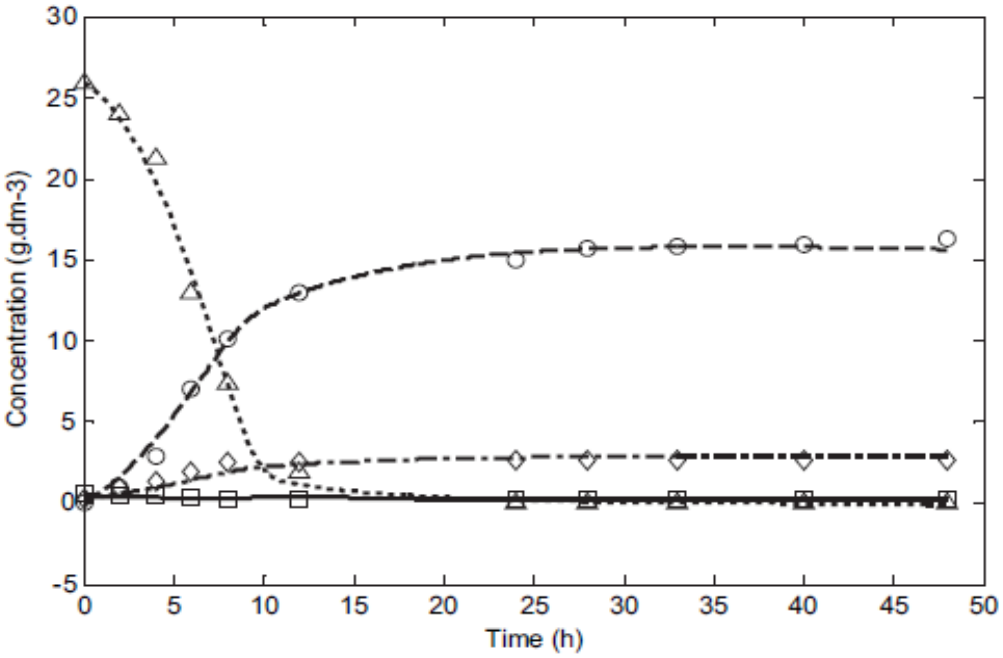

Figure 11. Change in concentrations of cellobiose, glucose, cell and ethanol against time. The experimental data are plotted with symbols while the simulated curves are shown in lines. Cellobiose is represented by (□) and solid line, glucose is represented by (Δ) and dotted line, cell is represented by (◊) and dash-dot line, and ethanol is represented by (○) and dash line. Operating conditions: C_o = 40 g/dm³, X_1 = 0.3 g/dm³, e_o = 4 g/dm³, and G_o = B_o = E_o = 0 [22].

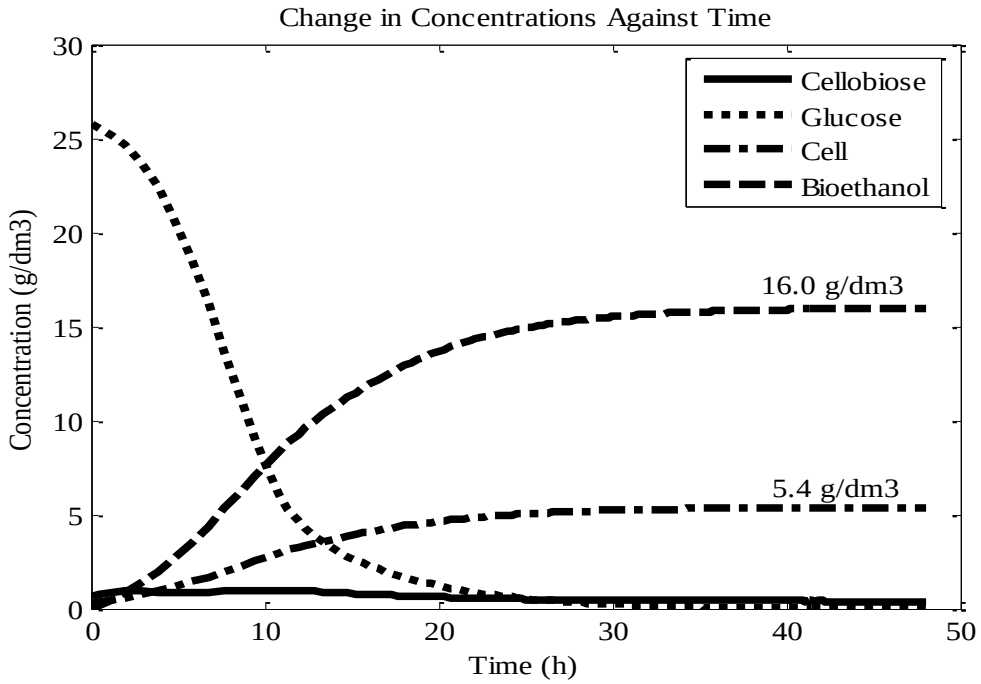

Figure 12: Change in concentration of cellobiose, glucose, cell and ethanol against time. Operating conditions: C_o = 40 g/dm³, X_1 = 0.3 g/dm³, e_o = 4 g/dm³, and G_o = B_o = E_o = 0.

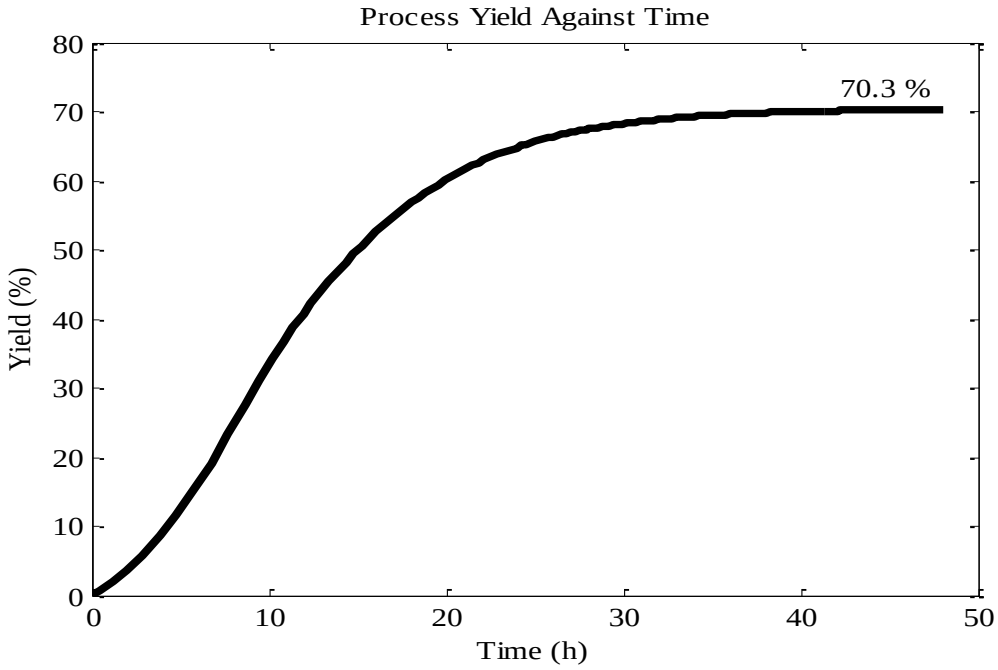

Figure 13: The response of process yield against time. (Yield = $\frac{0.9\,E}{0.511\,C_o} \times 100$)

The model developed is capable to capture the nonlinear behaviour of the bioethanol fermentation reactor. The verification step acts as the green light that affirms the accuracy of the process model for further control procedures. Since the fed-batch process model was also simulated using mechanistic equations developed by [22] and with the same values for the process parameters, the fed-batch process model was as accurate as the batch process model. Furthermore, the response of bioethanol concentration with different dilution rates for the fed-batch operation has demonstrated the accuracy of the fed-batch process model as well.

3.3. Feedforward Artificial Neural Network (FANN) Model Development

Conventional direct concentration measurement is cumbersome, expensive and time-consuming. Therefore, for online control with an accurate process model, concentration can be estimated and predicted. The concentrations could be easily estimated with the neural network structure that employs feedback of the concentrations, incorporating an accurate process model. In this section, a feedforward artificial neural network (FANN) is developed based on the fed-batch process where the ultimate target is to obtain a dynamic FANN model, which is able to describe the variation of bioethanol concentration as a function of (a) concentration of cellulose; and (b) concentration of cellulose and dilution rate.

3.3.1. Feedforward Artificial Neural Network Modelling of Fed-Batch Operating Mode

Nine different batches of data were generated from the simulation of the mechanistic model of the fed-batch operation of SSSF 24 of bioethanol production. The data are generated by varying the input cellulose concentration from 20 – 70 g/dm^3 and the dilution rate from 0.01 – 0.40 h^{-1} over a period of time of 48 hours for each change in input(s).

Then, these nine batches of data are divided to give five sets of data for training (Batch 1, 3, 5, 7 and 9), two sets for testing (Batch 2, and 6) and two sets for validation (Batch 4 and 8). The data for network training and testing corresponded to approximately 78%, while the rest were for network validation. The training method is according to the Levenberg-Marquart algorithm. Three different MISO models were developed for the fed-batch operation: (a) 3 inputs: the current value of input cellulose concentration, C(t), the current value of dilution rate, D(t), and the past value of bioethanol concentration, E(t-1), and 1 output: bioethanol concentration; (b) 2 inputs: the current value of cellulose concentration, C(t), and the past value of bioethanol concentration, E(t-1), and 1 output: bioethanol concentration; and (c) two inputs: the current value of dilution rate, D(t), and the past value of bioethanol concentration E(t-1), and 1 output: bioethanol concentration. The sum of squared error and coefficient of determination (R^2) values for the different number of neurons in the one hidden layer architecture for all three FANN models are given in Table 1.

Table 1. The sum of squared error (SSE) and coefficient of determination (R^2) values for the different numbers of neurons in one hidden layer. (a) Three inputs: C(t), D(t), and E(t-1); (b) Two inputs: C(t), and E(t-1); and (c) Two inputs: D(t), and E(t-1).

(a)

No. of Neuron(s)	Sum Squared Error (SSE)			Overall R^2(Training, Testing, Validation)
	Training	Testing	Training + Testing	
1	1.7414	0.2143	1.9557	0.9946
2	1.6646	0.1794	1.8440	0.9946
3	191.9539	85.0160	276.9699	0.0109
4	0.7848	0.4547	1.2395	0.9541
5	1.1533	8.9462	10.0995	0.8534
6	13.8908	3.5725	17.4633	0.9498
7	8.1402	10.2042	18.3444	0.8983
8	1.2611	0.7213	1.9824	0.9258
9	0.1548	0.1051	0.2599	0.9960
10	**0.0656**	**0.1696**	**0.2352**	**0.9988**
11	0.3486	0.6758	1.0244	0.9952
12	0.0826	0.0473	0.1299	0.7672
13	0.3713	22.5198	22.8911	0.7704
14	0.0450	5.1390	5.1840	0.7623
15	25.8871	3.2911	29.1782	0.9103
16	48.3839	28.3438	76.7277	0.6554
17	37.2079	45.7925	83.0004	0.6191
18	16.2217	3.9668	20.1885	0.8776
19	14.0725	11.7834	25.8559	0.7167
20	0.1601	7.6585	7.8186	0.5041

(b)

No. of Neuron(s)	Sum Squared Error (SSE)			Overall R^2 (Training, Testing, Validation)
	Training	Testing	Training + Testing	
1	1.6782	0.2251	1.9033	0.9944
2	31.1202	7.6066	38.7268	0.8292
3	1.2391	1.1887	2.4278	0.9906
4	25.0008	3.2896	28.2904	0.8862
5	61.3549	48.3302	109.6851	0.2252
6	2.7604	1.1937	3.9541	0.5825
7	**1.6409**	**0.2077**	**1.8486**	**0.9958**
8	2.8256	7.1936	10.0192	0.8490
9	0.8466	16.1876	17.0342	0.9357
10	2.3367	49.0229	51.3596	0.6900
11	1.0623	11.0712	12.1335	0.6173
12	1.3369	42.7341	44.0710	0.7517
13	45.3042	6.1139	51.4181	0.6311
14	55.8478	20.2423	76.0901	0.4083
15	77.7152	14.6387	92.3539	0.6701
16	3.4703	2.0583	5.5286	0.7677
17	1.5665	5.6535	7.2200	0.8998
18	3.0364	2.6797	5.7161	0.9136

19	13.8217	0.7935	14.6152	0.8840
20	1.0600	14.7007	15.7607	0.6276

(c)

No. of Neuron(s)	Sum Squared Error (SSE)			Overall R^2 (Training, Testing, Validation)
	Training	Testing	Training + Testing	
1	1.6740	0.1813	1.8553	0.9946
2	1.1475	0.2001	1.3476	0.9962
3	0.1621	0.1089	0.2710	0.9990
4	0.0629	0.0164	0.0793	0.9994
5	0.4769	0.2254	0.7023	0.9972
6	0.0485	0.2459	0.2944	0.9988
7	0.0427	0.2017	0.2444	0.9990
8	0.0781	0.0309	0.1090	0.9994
9	0.0520	0.0253	0.0773	0.9994
10	0.0409	0.0782	0.1191	0.9994
11	0.0473	0.0449	0.0922	0.9994
12	0.0575	0.0268	0.0843	0.9994
13	0.6613	1.2636	1.9249	0.9930
14	0.0527	0.2323	0.2850	0.9988
15	**0.0443**	**0.0065**	**0.0508**	**0.9998**
16	0.0194	0.0357	0.0551	0.9996
17	0.0380	0.1258	0.1638	0.9992
18	0.0565	0.0955	0.1520	0.9992
19	0.0501	0.1989	0.2490	0.9990
20	0.5648	1.7456	2.3104	0.9926

It is seen that the best network architecture for (a) 3 – 10 – 1, with SSE of 0.2352 and overall R^2 value of 0.9988, (b) 2 – 7 – 1, with SSE of 1.8486 and overall R^2 value of 0.9958, and (c) 2 – 15 – 1, with SSE of 0.0508 and overall R^2 value of 0.9998. The plot of SSE for the different number of neurons for conditions (a), (b) and (c) is as shown in Figure 14.

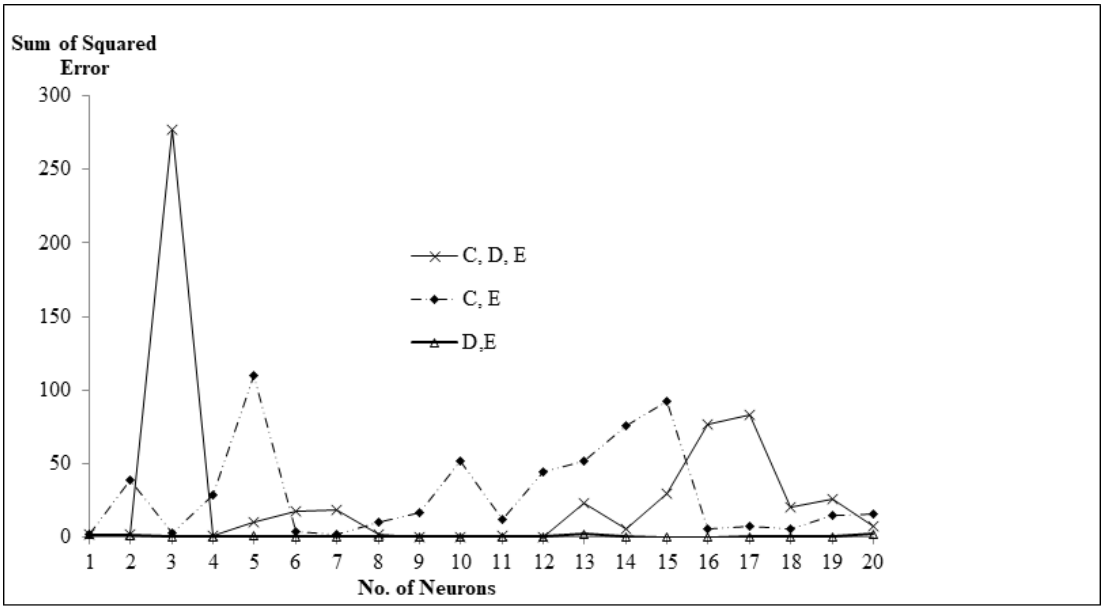

Figure 14. Comparison between three different conditions of inputs for network training, testing, and validation: (a) three inputs: cellulose concentration (C), dilution rate (D) and historical data of bioethanol concentration (E); (b) two inputs: cellulose concentration (C) and historical data of bioethanol concentration (E); and (c) two inputs: dilution rate (D) and historical data of bioethanol concentration. (E).

The result shows that the performance of the network architecture training using condition (c) is the best in terms of having the least SSE value and high regression value. This implies that the networks with dilution rate data are significant and highly related to the output (bioethanol concentration). Even though the networks under condition (a) are also trained with the dilution rate data, the additional input of cellulose concentration might reduce the network generalization capability. Zhang and Morris [30] mentioned the deterioration of the neural network generalization capability due to over-parametrization. Furthermore, it is easier and less time consuming to train the model with less input or only significant input towards the output. Therefore, it is shown that the selection of input significantly contributes to the performance of the network or output. Increasing the number of inputs will increase the complexity of the network structure. Careful selection and pairing of input-output for network training, testing and validation are required to obtain the most excellent neural network performance.

3.4. Feedforward Artificial Neural Network– Model Predictive Control (FANN_MPC) of Fed-Batch SSSF 24 of Bioethanol Production Model Development

The fed-batch process is a more preferred operation mode for the production of higher added-value products whereas in this study the fed-batch operating mode of SSSF 24 of bioethanol production. The fed-batch operating mode is also described for its higher yield in comparison to the batch or continuous operating modes [31]. Therefore, in the final stage of this study, a control system for the fed-batch operation was developed. The neural network–model prediction of the FANN-MPC was selected because of the enormous advantageous properties of both neural network and MPC. The neural network can be integrated as the internal model in an advanced nonlinear model predictive control algorithm [27]. This integration will decrease the complexity of the model required and make the computational process much simpler and faster than the nonlinear MPC technique.

The Matlab™ Simulink environment provides a controller block, the neural networks (NN) Predictive Control, which enables users to identify and train the neural network plant model to represent the dynamics of the plant. Then, the plant model will be used by the controller to predict the future performance. The FANN models identified in Section 3.3.1 will be imported into the controller, skipping the plant identification and network training steps in the NN Predictive Control block. The FANN-MPC model is shown in Figure 15.

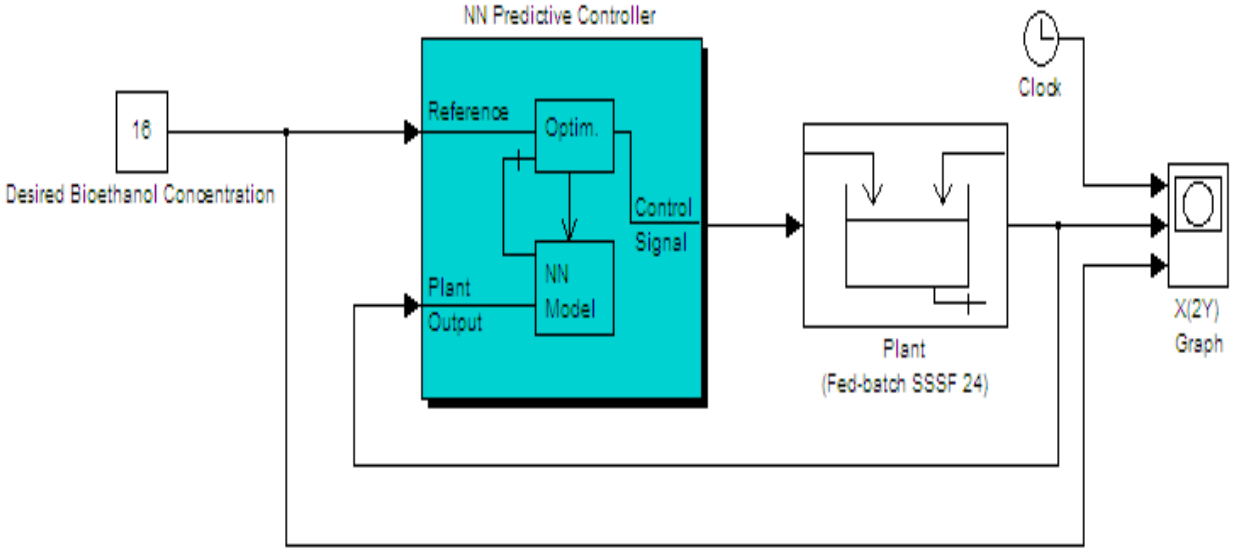

Figure 15. NNMPC model in the Simulink GUI environment.

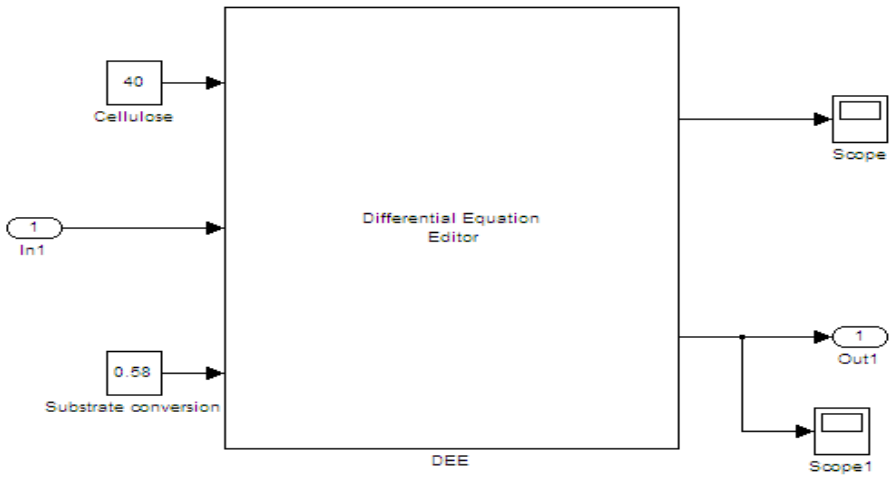

Figure 16. The embedded subsystem of the fed-batch operating mode of SSSF 24.

The reference for the controller system is the setpoint, in this case, the desired output of bioethanol concentration was set at 16 g/dm^3, which was according to the initial investigation by Shen and Agblevor [22] on the optimum bioethanol concentration able to be attained by the batch system. The 'Plant' refers to the embedded subsystem as shown in Figure 16, which was the modification of the mechanistic process model for the fed-batch of SSSF 24 shown in Figure 7. The neural network was generated and trained in the plant identification step. For the network architecture, the parameters including the size of the hidden layer, sampling interval, number of plant inputs delay, and number of plant outputs delay were set at 15, 10 s, 2 and 2, respectively. The number of nodes for the hidden layer was fixed at 15 as the results from the previous neural network modelling from Section 3.3.1 showed that the architecture 2 – 15 – 1 has the least SSE value and the highest R^2 when the number of hidden nodes was varied in between 1 to 20.

The selected input variable for the development of the FANN-MPC strategy was the dilution rate. The dilution rate has been identified as a significant input variable that can be manipulated to obtain the targeted output of bioethanol concentration even with any variation in input cellulose concentration. Since the dilution rate, which consists of the ratio between feed flow rate and culture volume, cannot be zero. If zero, no in-flow of feed was observed.

As from the research in [22] on the continuous operating mode of SSSF 24, the bioethanol concentration produced was highest when the dilution rate is at 0.04 h^{-1} and lowest near the washout point, where the dilution rate is at 0.4 h^{-1}. If the dilution rate is increased above μ_{max}, or the maximum growth rate of microorganisms (in this study it refers to the yeast/cell), a complete washout of the cell will occur. Therefore, the logical dilution rate ranged from a minimum of 0 (when no input or at the beginning of the process startup) to a maximum of 0.4 h^{-1} (near washout point). For the range of process output, it would be best if the training of the network could cover a wide range of data as shown in Section 3.3.1. Therefore, the rational range for the output bioethanol concentration was fixed between 0 – 15 g/dm^3.

Table 2. Values of NNMPC parameters.

Parameters	Value
Prediction horizon, N_2	6
Control horizon, N_u	2
Weighting parameter, ρ	0.5
Search parameter, α	0.4

There are four tuning parameters for the FANN-MPC as shown in Table 2. These parameters were tuned in order to obtain an assured prediction by the controller. The number of time steps over which the prediction errors are minimized, N_2, was set at 6, and the number of time steps over which the control increments are minimized, N_u, was set at 2. The control weighting factor, ρ, which will be multiplied by the sum of squared control increments in the performance function was set at 0.5. The final tuning parameter, the search parameter, α, determines when the line search was set at 0.4. In

addition to those tuning parameters, *"csrchbac"* was selected as the minimization routine. The minimization routine serves to compute the control signals that optimize future plant performance, and the *"csrchbac"* selected is a one-dimensional minimization using the backtracking method. Two iterations were performed per sample time. Table 2 summarized the values of FANN-MPC parameters used in this study.

3.4.1. Setpoint Tracking

Figure 17 below shows the results from the FANN-MPC system. It is observed that the response from the plant output has a settling time of around 70 hours. In comparison, the settling time without incorporation of NNMPC is around 150 hours, as seen in Figure 17. Even though the incorporation of FANN-MPC to the fed-batch system is able to reduce the settling time, this settling time is still considered very lag. Therefore, if the operator required a high concentration of bioethanol, the extraction of the product should be done at an early stage, at t around 47 hours, rather than waiting for the system to settle down. However, if the concentration of the product at a steady state is tolerable, the extraction of the product can be done any time after t = 47 hours. For a manual system, less manpower is required if the extraction period is longer, but this, in turn, had to sacrifice the product yield.

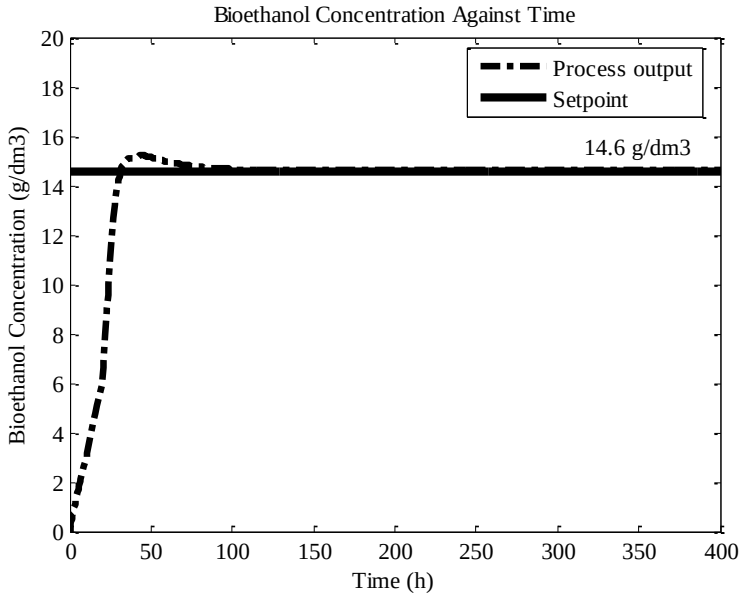

Figure 17. Response of the plant output with the incorporation of FANN-MPC.

In order to further check the ability to track the setpoint of the controller developed, the setpoint was changed from a constant value block to three different step response blocks. The first step change involved the rise of the setpoint from 5 g/dm^3 to 12 g/dm^3 at t = 100 hours; the second step change was a reduction of bioethanol concentration to 2 g/dm^3 at t= 250 hours, and the last step change involved the increment of setpoint to 15 g/dm^3. The result of these changes is shown in Figure 18. It is seen that the response of the process output fluctuated around the three setpoints. The process output requires approximately 50 hours to reach these setpoints. Therefore, again it is suitable to do the product extraction straight around t = 50 hours. The NNMPC controller is said to demonstrate a good ability in setpoint tracking. The response of the MV is shown in Figure 19. The FANN-MPC is able to modify different dilution rate values accordingly to the required MV. For the low setpoint, the MV was high and for a high setpoint of bioethanol concentration at 15 g/dm^3, the MV was reduced until 0.03 h^{-1}. The change in cell concentration for these changes is shown in Figure 20. The response of cell concentration is appropriate, whereby a high cell concentration is required to produce a high ethanol concentration. The relationship between bioethanol concentration and the cell concentration is directly proportional, while the bioethanol concentration is inverse proportional to the dilution rate.

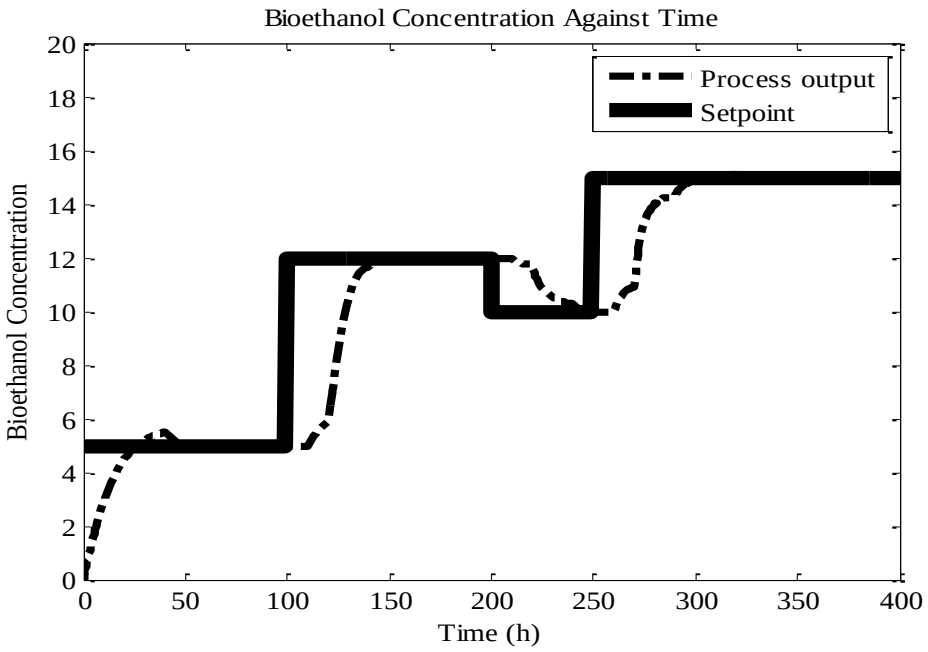

Figure 18. Response of the process output under setpoint changes.

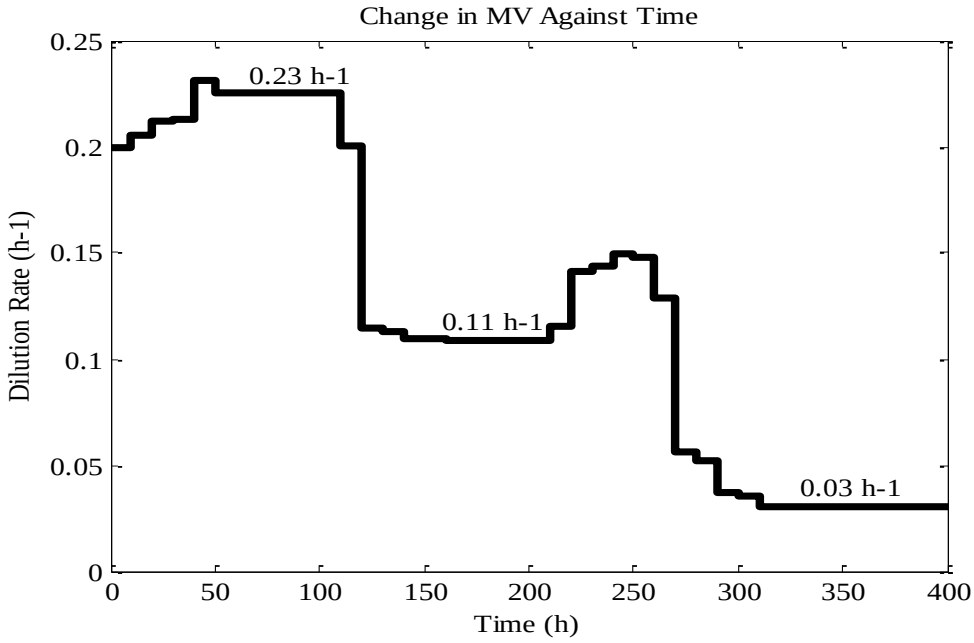

Figure 19. Response of the manipulated variable under setpoint changes.

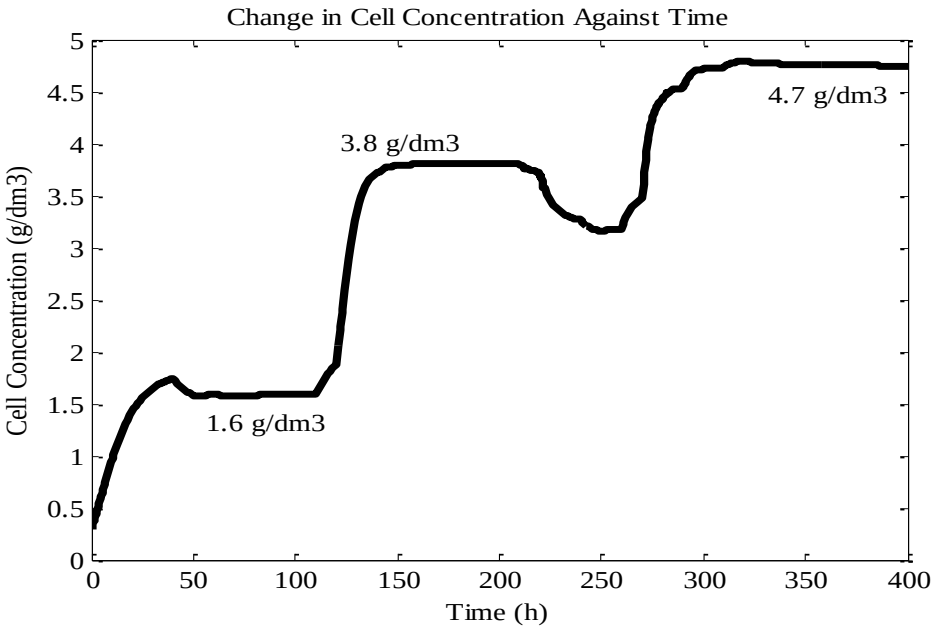

Figure 20. Response of the cell concentration under setpoint changes.

4. Conclusions

The nonlinearity in bio-processes caused hardship in modelling studies. The non-linearity was mainly caused by the fluctuation in feed quality and the sensitivity of microorganisms towards changes in operating conditions. Therefore, in this study on the bioethanol fermentation process from semi-simultaneous saccharification and fermentation (SSSF) process involving the usage of yeast, the Saccharomyces cerevisiae, a simple first-principle process model was simulated, which will reduce the complexity and time for modelling nonlinear process. Then, in order to improve the modelling process, the Feedforward artificial neural network (FANN) model was developed. FANN poses the ability to learn from historical process inputs-output data and the ability to capture the nonlinear behaviour of the biological system. In the final part of this study, a FANN-MPC strategy was developed to control the SSSF process.

There are promising aspects in the usage of the FANN to model the SSSF process. The employment of FANN-MPC is able to improve the bioethanol and cell concentrations of the fed-batch operation of the SSSF 24 process. The controller is able to give good performance under setpoint change. The main conclusion of this study are: -

a) Simulation of the process model to represent the dynamics of the actual process

- Mechanistic process models for fed-batch operating modes of SSSF 24 were simulated using the mechanistic equations (ODEs) modelled by [22]. These process models were used to generate data for training, testing and validation of the neural network.

b) Feedforward Artificial Neural Network (FANN) modelling of SSSF 24

- Multiple Input Single Output (MISO) neural network model for fed-batch operating modes of SSSF 24 was developed.
- The modelling with the neural network presents very promising results with a low SSE of 0.0508 and a high R^2 value of 0.9998, which is desirable for further development of the control system.
- The inadequacy in providing actual input data did not influence the modelling process by FANN. The availability of a mechanistic model is sufficient.
- The dilution rate was identified as a significant parameter that influences the process output. The neural model with two inputs: dilution rate and historical data from bioethanol concentration gave the lowest overall SSE values and R^2 value = ~ 1.0, irrespective of the number of neurons.

c) Development of FANN-MPC for fed-batch operating mode of SSSF 24

- It is seen that the input cellulose concentration parameter, inherently selected as the disturbance variable, has a strong influence on the controlled variable. Other than that, the cell concentration is also an important variable that required optimization and control as well. This brings to mind that the operation of FANN-MPC required thorough studies on the inputs-outputs pairing and correct selection of input variables.

Acknowledgements: The author would like to thank Universiti Sains Malaysia (USM) for providing the RUI grant PJKIMIA/8014100.

References

1. Mason, J. E. World energy analysis: H_2 now or later? *Energy Econ.* **2007**, *35*, 1315-1329.
2. Leblond, D. IEA: fossil energy to dominate market through 2030. *Oil & Gas J.* **2006**, *104*, 28-29.
3. EIA. *Annual Energy Outlook 2021*. Washington: Energy Information Administration **2021**. Available online: https://www.eia.gov/outlooks/aeo/ (accessed on 01/12/2021).
4. Rosegrant, M. W.; Msangi, S.; Sulser, T.; Valmonte-Santos, R.; Hazell, P.; & Pachauri, R. K. Biofuels and the global food balance: bioenergy and agriculture promises and challenges. *International Food Policy Research Institute (IFPRI) Focus 14* **2006**.
5. Abbasi, T.; Abbasi, S. A. Biomass energy and the environmental impacts associated with its production and utilization. *Renew. Sust. Energ. Rev.* **2010**, *14*, 919-937.
6. Osarhiemhen, A.; Augustine, O. A.; Oluranti, A; Francis, B.E. A review on the sustainable energy generation from the pyrolysis of coconut biomass. *Scientific African* **2021**, 13, e00909.
7. Muradov, N. Z.; Veziroglu, T. N. "Green" path from fossil-based to hydrogen economy: An overview of carbon-neutral technologies. *Int. J. Hydrog. Energy* **2008**, 33, 6804-6839.
8. Karpan, B.; Abdul Raman, A. A.; Taieb Aroua, M. K. Waste-to-energy: Coal-like refuse derived fuel from hazardous waste and biomass mixture. *Process Saf Environ Prot*. **2021** 149, 655-664.
9. Gajalakshmi, S.; Abbasi, S. A. Solid waste management by composting: state of the art. *Crit Rev Environ Sci Technol.* **2008**, 38, 311-400.
10. Volk, T. A.; Abrahamson, L. P.; Nowak, C. A.; Smart, L. B.; Tharakan, P. J.; White, E. H. The development of short-rotation willow in the northeastern United States for bioenergy and bioproducts, agroforestry and phytoremediation. *Biomass Bioenergy* **2006**, 30, 715-727.
11. Tuskan, G. A.; Difazio, S.; Jansson, S.; Bohlmann, J.; Grigoriev, I.; Hellsten, U. The genome of black cottonwood, Populus trichocarpa (Torr. & Gray). *Science* **2006**, 313, 1596-1604.
12. Geyer, W. A. Biomass production in the Central Great Plains USA under various coppice regimes. *Biomass Bioenergy* **2006**, 30, 778-783.
13. Parrish, D. J.; Fike, J. H. The biology and agronomy of switchgrass for biofuels. *Crit Rev Plant Sci.* **2005**, *23*, 423-459.
14. Hallam, A.; Anderson, I. C.; Buxton, D. R. Comparative economic analysis of perennial, annual, and intercrops for biomass production. *Biomass Bioenergy* **2001**, 21, 407-424.
15. Lewandowski, I.; Scurlock, J. M. O.; Lindvall, E.; Christou, M. The development and current status of perennial rhizomatous grasses as energy crops in the US and Europe. *Biomass Bioenergy* **2003**, *25*, 335-361.
16. Heaton, E.; Voight, T.; Long, S. P. A quantitive review comparing the yields of two candidate C4 biomass crops in relation to nitrogen, temperature and water. *Biomass Bioenergy* **2004**, 27, 21-30.
17. Flevaris, K.; Chatzidoukas, C. Optimal fed-batch bioreactor operating strategies for the microbial production of lignocellulosic bioethanol and exploration of their economic implications: A step forward towards sustainability and commercialization. *J. Clean. Prod***. 2021**, 295, 126384.
18. Devi, A.; Singh, A.; Bajar, S.; Pant, D.; Ud Din, Z. Ethanol from lignocellulosic biomass: An in-depth analysis of pre-treatment methods, fermentation approaches and detoxification processes. *J. Environ. Chem. Eng.* **2021**, 9(5), 105798.
19. Haeun, Y.; Ha, E.B.; Dongho, H.; Jay, H.L. Reinforcement learning for batch process control: Review and perspectives. *Annu Rev Control* **2021**, in press.
20. Feng, X.; Yu, T.; Wang, J. L. Nonlinear GPC with In-place Trained RLS-SVM Model for DOC Control in a Fed-batch Bioreactor. *Chin. J. Chem. Eng.* **2021**, 20 (5), 988-994.

21. Petre, E.; Selişteanu, D.; Roman, M. Advanced nonlinear control strategies for a fermentation bioreactor used for ethanol production. *Bioresour. Technol.* **2021** 328, 124836.
22. Shen, J.; Agblevor, F. A. Modelling semi-simultaneous saccharification and fermentation of ethanol production from cellulose. *Biomass Bioenergy* **2010**, *34*(8), 1098-1107.
23. Meleiro, L. A.C.; Zuben, F. J. V.; Filho, R. M. Constructive learning neural network applied to identification and control of a fuel-ethanol fermentation process. *Eng. Appl. Artif. Intell.* **2009**, *22*, 201-215.
24. Ahmad, Z.; Zhang, J. Combination of multiple neural networks using data fusion techniques for enhanced nonlinear process modelling. *Comput. Chem. Eng.* **2005**, *30*, 295-308.
25. Jayalakshmi, T.; Santhakumaran, A. Statistical normalization and backpropagation for classification. *International Journal of Computer Theory and Engineering* **2011**, *3*(1), 1793-8201.
26. Lera, G.; Pinzolas, M. Neighbourhood-based Levenberg-Marquardt algorithm for neural network training. *IEEE Transactions on Neural Networks* **2002**, *13*(5), 1200-1203.
27. Nagy, Z. K. Model-based control of a yeast fermentation bioreactor using optimally designed artificial neural networks. *Chem. Eng. J.* **2007**, *127*, 95-109.
28. The MathWorks, I. NN Predictive Control.
29. Vasickaninova, A.; Bakosova, M.; Meszaros, A.; Klemes, J. J. Neural network predictive control of a heat exchanger. *Appl. Therm. Eng.* **2011**, 1-7.
30. Zhang, J.; Morris, A. J. A sequential learning approach for single hidden layer neural networks. *Neural Netw.* **1998**, *11*(1), 65-80.
31. Chang Y.H., Chang K.S., Huang C.W., Hsu C.L., Janga H.D., Comparison of batch and fed-batch fermentations using corncob hydrolysate for bioethanol production, *Fuel,* **2012**, *97, 166-173.*